Desriping Hyperion Imagery Using Spline Interpolation

Fuan Tsai
Center for Space and Remote Sensing Research
National Central University
300 Zhong-Da Rd.
Zhong-Li, Taoyuan 320 Taiwan
ftsai@csrsr.ncu.edu.tw

Shi-Qi Lin, Jiann-Yeou Rau, Liang-Chien Chen, Gen-Rong Liu
Center for Space and Remote Sensing Research
National Central University
300 Zhong-Da Rd.
Zhong-Li, Taoyuan 320 Taiwan

Abstract: This paper presents an alternative approach for removing striping patterns of Hyperion hyperspectral imagery. In this study, a cubic spline-based curve-fitting algorithm was used to estimate gray values of striping pixels in an image. The idea is to treat each line of a Hyperion image as a piece-wise spline curve in each spectral band. After identifying pixels affected by the striping noises, the noise-free pixels are collected and used as samples to construct a cubic Hermite spline curve that passes all of the control points (samples). The original gray values of striping covered pixels can then be approximated from the spline curve. Applying this procedure to an image line by line or column by column, a striping-free image can be reconstructed accordingly.
Keywords: image destriping, striping removal, spline, curve fitting

1. Introduction

Hyperion is currently the only available source of satellite hyperspectral remote sensing. Like many other imaging instruments with multi-detectors, Hyperion imagery exhibits various degrees of striping patterns (banding noise) in some of its bands due to variations in sensor calibration, for example, the dark current imbalances (DC Bias) of the detectors across the pixel direction of the detector (Dykstra and Segal, 1985). Similar pronounced striping patterns are also noticed in other remote sensing data sets, such as LANDSAT MSS and TM images, SPOT imagery, and even in non-image format data sets. Researchers have developed a few algorithms and procedures to eliminate or reduce these artifacts. In the early days, the most commonly adopted destriping method is probably the histogram modification algorithm (Horn and Woodham, 1979) or histogram matching (Wegener, 1990). As remote sensing technologies advance, more sophisticated methods have also been developed to deal with this problem. For example, Chander et al. (2002) used inversed regression functions to reducing the striping in Landsat TM Band-6 data; Aizenberg and Butakoff (2002) developed a filter in the frequency domain, which works well for removing periodic noise. For non-image data, Oimeoen (2000) employed low-pas and high-pass filters alternately to isolate and remove stripes from digital elevation model (DEM) data. Similar technique was further developed into a spatial filter specifically designed for the removal of striping artifacts in DEMs (Albani and Klinkenberg, 2003).

Although these methods all seem to produce novel results, most of them were designed for specific senors or data types and may not be suitable for other data. More seriously, they may lead to loss or degradation of data quality and other side-effects, if applied blindly to Hyperion images. As mentioned earlier, the stripping artifacts of Hyperion imagery is primarily caused by dark current bias, which is commonly seen in data acquired with push-broom (area array) sensors, (for example, AIS or Hyperion). A model was established to remove the striping patterns of airborne push-broom imaging spectrometer data (Dykstra and Segal, 1985; Kruse, 1988). Similar algorithm has been modified to handle space-borne Hyperion data (Kruse, 2002). Their approach involves in adjusting pixel gray values column by column (for all bands) according to a calculated offset relative to the scene average. Others also developed statistics-based "local" destriping algorithms for Hyperion imagery (Datt et al., 2003). Their methods both seem provide reasonable detriping results without introducing too much undesired side-effects. However, both algorithms require a full examination of the whole scene in order to obtain necessary statistical parameters for local adjustment. This study investigated and developed an alternative approach for removing striping noise and reconstructing missing information of Hyperion images based on a cubic spline interpolation technique, which in a way requires only a prior knowledge on the positions of the striping columns.

2. Spline-based Image Processing

Mathematically, spline refers to a piecewise function consisting of polynomial pieces. It is commonly used to describe curves and surfaces in computer-aided design and related fields. For signal and image processing, spline interpolation has been considered a useful tool and been used intensively in various tasks (Unser, 1999). Some examples of spline-based image processing include image compression (Torichi et al., 1988), interpolation (Unser et

al. 1991) and image registration (Jonic et al., 2001; Pluim et al., 2000). Park and Sang (1999) also employed a two-dimensional non-uniform rational B-spline approach to reconstruct missing data from corrupted images.

For a cubic spline, the curve will maintain a C^2 continuity, meaning that the second derivatives are continuous. For this study, cubic Hermite spline is used to construct gray values of pixels affected by striping noise from neighboring pixels. The idea is to treat each row of samples in a Hyperion image as a cubic spline with uniform parametric sampling. However, for pixels affected by striping noise, they should be removed and the rest of the samples form a set of control points to construct the spline passing through all control points. For the i-th segment of the spline curve passing through *n+1* control points ($P_0 \sim P_n$), it can be described as the following equation:

$$P_i(u) = < h_1(u), h_2(u), l_i h_3(u), l_i h_4(u) > \begin{Bmatrix} P_{i-1} \\ P_i \\ P_{i-1}^u \\ P_i^u \end{Bmatrix} \qquad (1)$$

where l_i is the chord-length of the curve segment and $h_1(u) \sim h_4(u)$ are the four Hermite polynomials for u = [0,1]:

$$\begin{aligned} h_1(u) &= 2u^3 - 3u^2 + 1 \\ h_2(u) &= -2u^3 + 3u^2 \\ h_3(u) &= u^3 - 2u^2 + u \\ h_4(u) &= u^3 - u^2 \end{aligned} \qquad (2)$$

Because the restriction of C^2 continuity, n-1 equations can be constructed by taking derivatives of Eq. (1) and (2). However, two more conditions are still needed in order to obtain all the tangents at the control points of the spline curve. A common technique to supply the extra conditions is to set the second derivatives at the beginning and ending points of the curve to zero, which results in a "natural" cubic spline. The complete system can be described as Eq. (3):

$$\begin{bmatrix} \frac{4}{l_1} & \frac{2}{l_1} & & & & \\ \frac{2}{l_1} & \frac{4}{l_1}+\frac{4}{l_2} & \frac{2}{l_2} & & & \\ & \frac{2}{l_2} & \frac{4}{l_2}+\frac{4}{l_3} & & & \\ & & & \cdots & & \\ & & & \frac{4}{l_{n-1}}+\frac{4}{l_n} & \frac{2}{l_n} & \\ & & & \frac{2}{l_n} & \frac{4}{l_n} & \end{bmatrix} \begin{Bmatrix} P_0^u \\ P_1^u \\ \cdots \\ P_n^u \end{Bmatrix} = 6 \begin{bmatrix} \frac{(P_1 - P_0)}{l_1^2} \\ \frac{(P_1 - P_0)}{l_1^2} + \frac{(P_2 - P_1)}{l_2^2} \\ \cdots \\ \frac{(P_{n-1} - P_{n-2})}{l_{n-1}^2} + \frac{(P_n - P_{n-1})}{l_n^2} \\ \frac{(P_n - P_{n-1})}{l_n^2} \end{bmatrix} \qquad (3)$$

As can be seen in Eq. (3), it has become a linear system, and can be solved efficiently using a number of numerical analysis algorithms. Once the tangents (first degree derivatives, P^u) of all control points are solved, pixels previously removed from the data list can be approximated from their adjacent points according to Eq. (1) and (2). In implementation, this study utilized the GNU Scientific Library (GSL) functions to perform spline-related computations.

3. Testing Results

The developed spline-based interpolation algorithm was tested on several digital photographs with man-mad striping noise and on selected noisy bands of a Hyperion image. Fig. 1 shows a digital photograph with periodic striping noise superimposed on it. The striping noise is one-pixel wide and repeated every 30 samples. The result of cubic spline interpolation is displayed in Fig. 2. As can be seen on Fig. 2, after the correction, the stripping covered lines are replaced with more reasonable gray values.

A similar test was also carried out on real Hyperion imagery. Fig. 3 shows the original data of Band-10 (447 nm) of a Hyperion hyperspectral image. In this figure, three dark vertical lines are pronounced. In addition, there are also less obvious stripes in the image, especially near the right edge of the image. After identifying the stripping columns, the developed cubic spline interpolation algorithm was employed to approximate the gray values of missing pixels row by row. The destriped result is demonstrated in Fig. 4. As displayed in the figure, the original dark vertical lines are removed and the striping pattern near the right edge has also been alleviated.

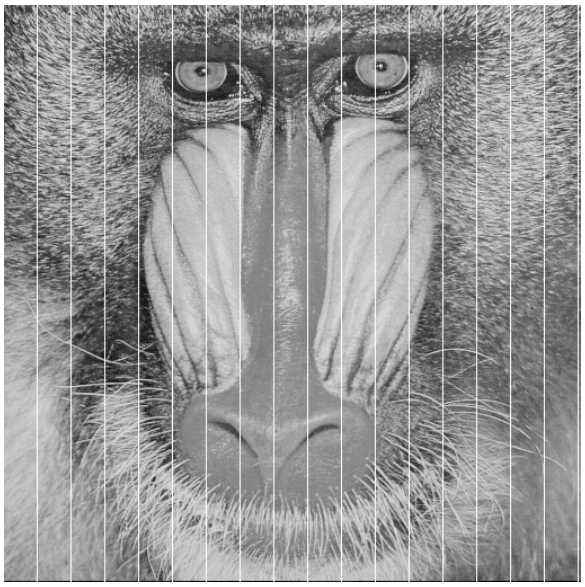

Fig. 1: Digital photography with single-pixel striping.

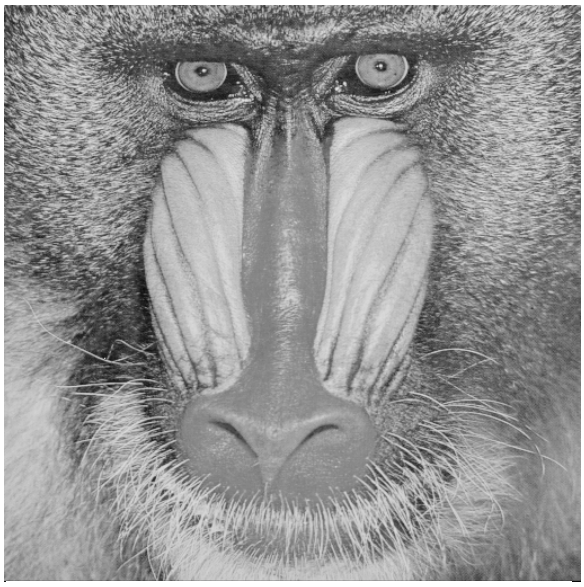

Fig. 2: Cubic spline destriping result of Fig. 1

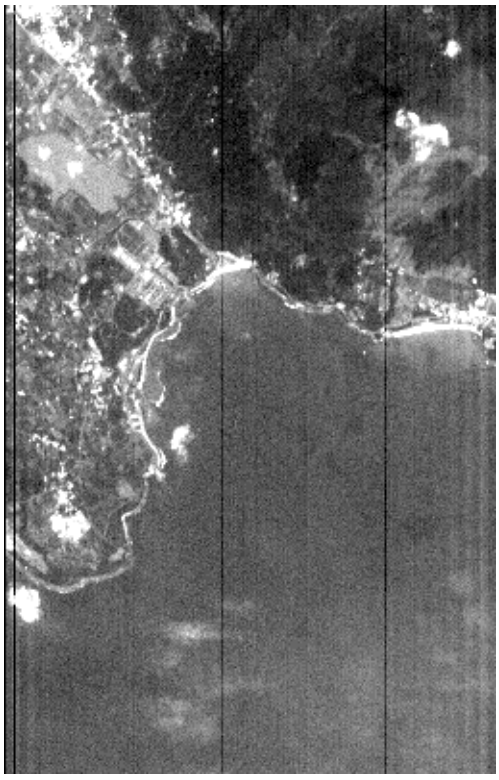

Fig. 3: Band-10 of a Hyperion Image.

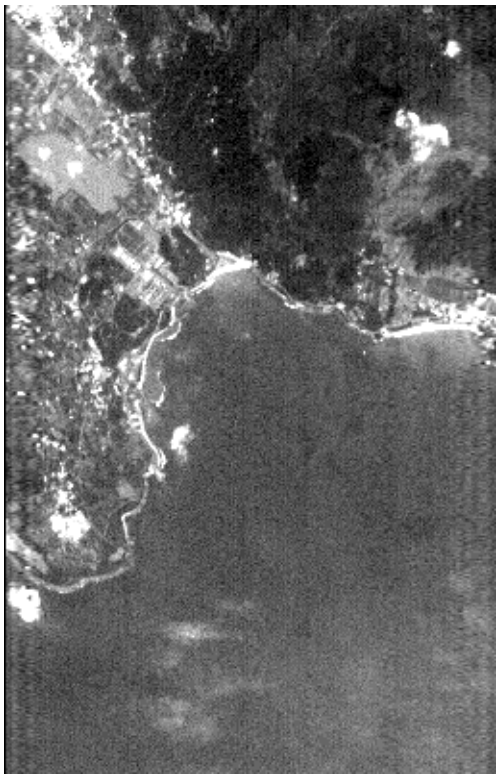

Fig. 4: Destriped result of band-10.

In some cases, the striping width may be more than one pixel, therefore, the developed destriping algorithm was also tested for handling multi-pixel striping patterns. Fig. 5 is the same digital photograph as Fig. 1, but the striping width has been increased to three pixels. The spline-based destriping algorithm also generates very good result (as displayed in Fig. 6). However, widening the striping pattern to five pixels, and the artifacts start to be noticeable after destriping (Fig. 7), although in general the procedure still recovers most of the missing pixels reasonably. Fig. 8 is another band (Band-192, 2073 nm) of the same Hyperion image displayed in Figure 3. In this wavelength region, Hyperion exhibits more serious striping patterns than shorter wavelength regions (probably due to low signal-to-noise ratio at shortwave infrared of Hyperion sensor). The same spline-based destriping procedure was applied to image and the result is displayed in Fig. 9. From Fig. 9, it is noticeable that the spline-based destriping approach has effectively clean up most of the noise (especially over the land), but in some areas, the destriping result shows similar artifact patterns as Fig. 7. The reason for this symptom and how to correct it is still under investigation and will be addressed in future work.

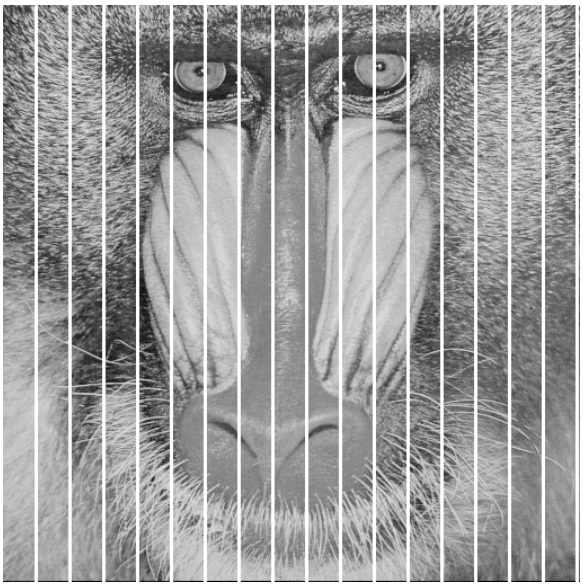

Fig. 5: Digital photograph with three-pixel-wide striping.

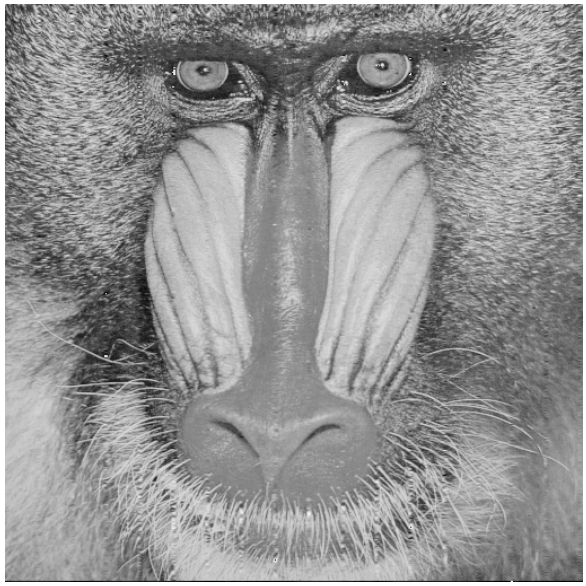

Fig. 6: Spline destriping result of Fig. 5.

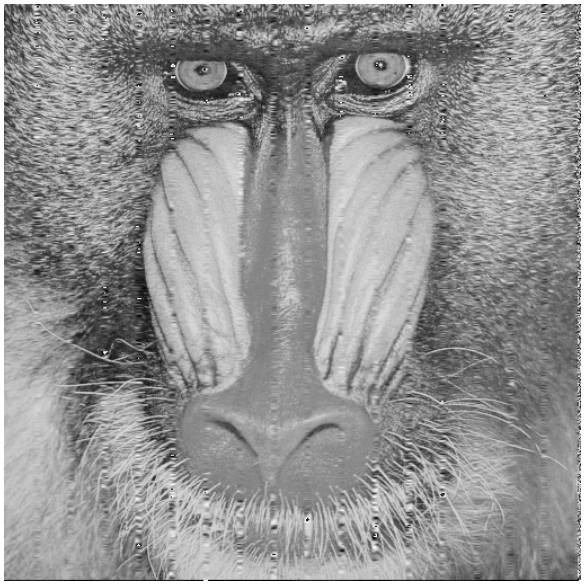

Fig. 7: Spline destriping result of 5-pixel wide stripes.

4. Conclusions and Future Work

This paper presents an alternative approach for remove or reduce the striping noise of Hyperion hyperspectral imagery. The developed algorithm is based on cubic spline interpolation to reconstruct the gray values of pixels affected by striping noise. Test examples demonstrate that the developed spline-based approach can effectively remove banding noise and reconstruct the image reasonably. Tests on two Hyperion bands also generated promising results. Compared to the original noisy Hyperion bands, the reconstructed images were clean and pixels previously covered by stripes were restored reasonably. In summary, the developed cubic spline interpolation algorithm is an effective approach for destriping Hyperion imagery.

The work presented in this paper is a preliminarily study. A few issues will be further investigated and continuously improved. For example, the mechanism to identify striping positions automatically. Also, the developed algorithm works excellent on single-pixel or narrow stripes, but may produce biased interpolations locally. This may require more sophisticated spline interpolation schemes, such as two-dimensional spline-surface interpolation and/or non-uniform spline models.

Fig. 8: Band-192 of a Hyperion image.

Fig. 9: Spline-based destriping of Fig. 8.

Acknowledgement

This study was supported in part by the National Science Council of Taiwan under projects NSC-94-2752-M-008-004-PAE and NSC-94-2211-E-008-031.

References

[1] Aizenberg, I. N. and Butakoff, C., 2002. Frequency domain medianlike filter for periodic and quasi-periodic noise removal, *Proc. SPIE Image Processing: Algorithms and Systems*, vol. 4667, pp. 181-191.

[2] Albani, M. and Klinkenberg, B., 2003. A Spatial Filter for the Removal of Striping Artifacts in Digital Elevation Models, *PE&RS*, 69(7), pp. 755-765.

[3] Chander, G., Helder, D.L. and Boncyk, W.C., 2002. LANDSAT—4/5 BAND 6 Relative Radiometry, *IEEE Trans. Geosciences & Remote Sensing*, 40(1), pp. 206-210.

[4] Datt, B., McVicar, T.R., Van Niel, T.G., Jupp, D.L.B., and Pearlman, J.S., 2003. Preprocessing EO-1 Hyperion hyperspectral data to support the application of agricultural indexes, *IEEE Trans. Geoscience and Remote Sensing*, 41(6), pp.1246-1259.

[5] Dykstra, J. D., and Segal, D. B., 1985. Analysis of AIS data of the Recluse Oil Field, Recluse, Wyoming: *Proceedings AIS workshop, 8-10 April, 1985, JPL Publication 85-41*, Jet Propulsion Laboratory, Pasadena, California, pp. 86-91.

[6] Horn, B.K.P., and Woodham, R.J., 1979. Destriping Landsat MSS Imagery by Histogram Modification, *Computer Graphics and Image Processing*, 10, pp. 68-83.

[7] Jonic, S., Thevenaz, P., Unser, M.A., 2001. Multiresolution spline-based 3D/2D registration of CT volume and C-arm images for computer-assisted surgery, *Proc. SPIE Medical Imaging 2001,* Vol. 4322, pp. 1101-1109.

[8] Kruse, F., 2002. Comparison of AVIRIS and Hyperion for Hyperspectral Mineral Mapping, *Proc. 11th JPL Airborne Geoscience Workshop*, 4-8 March 2002, Pasadena, California USA.

[9] Oimoen, M.J., 2000. An effective filter for removal of production artifacts in U.S. Geological Survey 7.5-minute digital elevation models, *Proc. of the Fourteenth International Conference on Applied Geologic Remote Sensing*, November, Las Vegas, N USAV, pp. 311-319

[10] Park, J.W., and Sang, U.L., 1999. Recovery of corrupted image data based on the NURBS interpolation, *IEEE Trans. Circuits and Systems for Video Technology*, 9(7), pp. 1003-1008.

[11] Pluim, JPW, Maintz, JBA, Viergever, MA, 2000. Image Registration by Maximization of Combined Mutual Information and Gradient Information, *Proc. Third International Conference on Medical Image Computing and Computer-Assisted Intervention, Lecture Notes In Computer Science*; Vol. 1935, 452-461

[12] Toraichi, K., Yang, K., Kamada, M., and Mori, R., 1988. Two-dimensional spline interpolation for image reconstruction, *Pattern Recognition*, 21(3), pp. 275-284.

[13] Unser, M., Aldroubi, A., Eden, M., 1991. Fast B-spline transforms for continuous image representation and interpolation, *IEEE trans. Pattern Analysis and Machine Intelligence*, 13(3), pp. 277-285.

[14] Unser, M., 1999. Splines: A perfect fit for signal and image processing, *IEEE Signal Processing*, 16(6), pp. 22-38.
[15] Wegener, M., 1990. Destriping multiple sensor imagery by improved histogram matching, *International Journal of Remote Sensing*, 11, pp. 859-875.